Anal Bioanal Chem (2005) 383: 41–47
DOI 10.1007/s00216-005-3355-5

ORIGINAL PAPER

Hans J. Nilsson · Tolek Tyliszczak · Richard E. Wilson
Lars Werme · David K. Shuh

Soft X-ray scanning transmission X-ray microscopy (STXM) of actinide particles

Received: 8 April 2005 / Revised: 22 May 2005 / Accepted: 24 May 2005 / Published online: 14 July 2005

Abstract A descriptive account is given of our most recent research on the actinide dioxides with the Advanced Light Source Molecular Environmental Science (ALS-MES) Beamline 11.0.2 soft X-ray scanning transmission X-ray microscope (STXM) at the Lawrence Berkeley National Laboratory (LBNL). The ALS-MES STXM permits near-edge X-ray absorption fine structure (NEXAFS) and imaging with 30-nm spatial resolution. The first STXM spectromicroscopy NEXAFS spectra at the actinide $4d_{5/2}$ edges of the imaged transuranic particles, NpO_2 and PuO_2, have been obtained. Radiation damage induced by the STXM was observed in the investigation of a mixed oxidation state particle (Np(V,VI)) and was minimized during collection of the actual spectra at the $4d_{5/2}$ edge of the Np(V,VI) solid. A plutonium elemental map was obtained from an irregular PuO_2 particle with the dimensions of 650 × 650 nm. The Pu $4d_{5/2}$ NEXAFS spectra were collected at several different locations from the PuO_2 particle and were identical. A representative oxygen K-edge spectrum from UO_2 was collected and resembles the oxygen K-edge from the bulk material. The unique and current performance of the ALS-MES STXM at extremely low energies (ca. 100 eV) that may permit the successful measurement of the actinide 5d edge is documented. Finally, the potential of STXM as a tool for actinide investigations is briefly discussed.

H. J. Nilsson · T. Tyliszczak · R. E. Wilson · D. K. Shuh (✉)
The Glenn T. Seaborg Center, Chemical Sciences Division, Lawrence Berkeley National Laboratory, One Cyclotron Road, Berkeley, CA 94720, USA
E-mail: DKShuh@lbl.gov

H. J. Nilsson · L. Werme
SKB, Box 5864, 10240 Stockholm, Sweden

R. E. Wilson
Nuclear Sciences Division, Lawrence Berkeley National Laboratory, One Cyclotron Road, Berkeley, CA 94720, USA

L. Werme
Department of Physics, Uppsala University, Box 530, 751 21 Uppsala, Sweden

Keywords Actinide · STXM · NEXAFS · Spectromicroscopy · Plutonium · Neptunium

Introduction

The emergence of microspectroscopic and fluorescence-based techniques has permitted investigations of actinide materials at sources of soft X-ray synchrotron radiation [1–5]. Spectroscopic techniques with fluorescence-based detection are particularly useful and have immediate utility for actinide investigations since they are sensitive to small amounts of material, and can be bulk sensitive, thereby avoiding complications of clean surface preparation and the accompanying safety considerations. A very recent complementary development along these lines has been the use of scanning transmission X-ray microscopy (STXM) spectromicroscopy to investigate small particles of actinide materials [6, 7]. STXM enables high-resolution near-edge X-ray absorption fine structure (NEXAFS) spectroscopy and imaging, both at the 30-nm length scale with thin sample materials [8, 9].

STXM is particularly amenable to studies of radioactive materials because it operates at ambient pressure thereby removing concerns about vacuum, uses fully sealed sample holders, and in theory only requires a tiny amount of sample material (e.g., a single particle of 10 fg). There are several actinide electron energy levels residing in the soft X-ray region, one of which is of particular utility for STXM . Also of particular relevance for actinides and soft X-ray STXM is the capability to probe the K-edges of the light elements such as carbon, nitrogen, and oxygen that are frequently involved in the chemical bonding in a range of actinide materials. An example of this is the actinide oxides and specifically, the actinide dioxides. Actinide dioxides are of great technological importance as nuclear fuel materials, in the long-term storage of excess defense materials, in the aging processes associated with weapons, and in the environmental transport of actinides [10]. Oxygen

K-edge NEXAFS is an excellent probe of the covalency of an actinide oxide bond, since actinide 5f/6d bonding with the O 2p forms an antibonding orbital weighted towards the actinide contribution [11].

This manuscript presents a descriptive account of our most recent, on-going actinide research, development, and results centered on the actinide dioxides at the Advanced Light Source Molecular Environmental Science (ALS-MES) Beamline 11.0.2 STXM of the Lawrence Berkeley National Laboratory (LBNL).

Experimental

The ALS-MES Beamline 11.0.2 is a 5.0-cm period elliptical-polarization undulator (EPU) beamline located at LBNL. The ALS-MES STXM resides on branchline 11.0.2.2, which has been optimized for STXM operations [6, 12, 13]. The combination of zone plates and the performance characteristics of the beamline provides a regular operational energy range of 120–2,160 eV. The appropriate choice of available zone plates and monochromator settings results in spatial resolution of better than 30 nm and a resolving power ($E/\Delta E$) of 5,000–7,500 for NEXAFS spectroscopy [14]. The ALS-MES STXM primarily functions in transmission and utilizes two transmission detectors. The first mode utilizes a photomultiplier with a scintillator detector and the second is a silicon photodiode. Currently, the STXM operates with higher count rate and substantially better signal to noise with photodiode detection. Further technical details about the ALS-MES beamline and STXM can be obtained from the ALS-MES website [15].

The ALS-MES STXM collects data in single-energy imaging, linescan, and multiple-energy image scans (stacks). In the two energy-dependent modes, lines or images are obtained with the energy being changed in a stepwise manner between each line or image acquisition. From these measurements, spectral information for a single position or selected area can be extracted. The ALS-MES STXM employs user-friendly control software. Data reduction and processing at the ALS-MES STXM is done almost exclusively with the axis program [16].

The ALS STXM samples are mounted on an indicated holder capable of accommodating four samples or sample packages. For radioactive materials, samples are safely and permanently enclosed between a pair of either 50-nm or 100-nm Si_3N_4 windows to form a suitable sample package. This permits the use of solid samples as well as wet or liquid samples. In the latter case, the sample volume must be small and preparation must be quick to avoid liquid evaporative loss. A prerequisite for general STXM samples is that they have an accessible thickness dimension of around a few hundred nanometers depending on the elemental cross-section, energy of the absorption edge, and local elemental concentration. Particle sizes of about 100 to 1,000 nm are generally suitable and sample materials are often ground to a fine powder to obtain particles of appropriate dimensions.

The actual application of radioactive material to the first Si_3N_4 window is done using a standard inspection microscope at 30 times magnification. A 2-cm human hair fiber fixed to a tantalum wire is used to gather particulates, which attach to the fiber and subsequently transfer the radioactive powder or paste to the surface of the window. Due to the malleability of the fiber, it is simply tapped directly onto the window. Once the particles have been distributed on the first window, another window is aligned with the first and is hermetically sealed along the edges with adhesive.

The materials employed in these initial studies were $^{238}UO_2$ obtained from Alfa–Aesar, $^{237}NpO_2$ from high-temperature inductive heating of a characterized dilute Np(V) solution prepared by standard methods at LBNL on a Pt counting plate under atmosphere, and low-fired (ca. 875 K) $^{242}PuO_2$ material obtained from Oak Ridge National Laboratory. These actinide oxides had nominal dioxide stoichiometry and were powdered as needed to obtain particles of suitable sizes for STXM experiments. The actinide dioxides utilized in this study have the fluorite-type face-centered (fcc) crystal structure. The mixed oxidation state Np(V,VI) salt was obtained from the solid residue of an uncharacterized Np(V) solution from which the solvent had evaporated and was slightly pink in appearance. The identification of the uncharacterized solid as 25% Np(V) and 75% Np(VI) is based on results from UV/Vis spectroscopy. This Np solid could be a mixed oxidation state single-phase compound or a two-phase material.

The actinide elements have several electron core levels that reside in the soft X-ray energy regime. The most well known of these actinide element thresholds are the $5d_{5/2,3/2}$ that lie in the range of 90–150 eV for the lighter actinides and have giant cross-sections [17]. However, there is currently no STXM that regularly operates at energies low enough to make use of these absorption edges. The regular energy range of the ALS-MES STXM encompasses the entire actinide N_{I-VII} edge series (4s, $4p_{1/2,3/2}$, $4d_{3/2,5/2}$, $4f_{5/2,7/2}$). The initial STXM investigations of uranium oxide particulates have shown that the $4d_{5/2}$ edge is the most useful absorption edge and in the case of uranium has a reproducible charge state shift of approximately 1.3 eV from uranium(IV) dioxide to uranium(VI) trioxide [6]. The actinide $4d_{5/2}$ spectra collected in this investigation are referenced to transmission from areas without actinide material, linear backgrounds are extracted, and the features are presented normalized to peak maximum. The overall actinide 4d absorption edge is broad (100–200 eV) with prominent white lines [18]. In the STXM measurements, only the leading white line is analyzed and shown. In this manuscript, this is referred to as the $4d_{5/2}$ edge (there is no multiplet structure). The energy resolution of the measurements is approximately 0.15 eV at the actinide edges and about 0.11 eV at the oxygen K-edge. All

images and NEXAFS spectra were recorded with horizontal EPU polarization.

Radioactive sample package holders were handled, loaded, unloaded, and the ALS-MES STXM certified as non-radioactive following the completion of the experiments. Small metal foil containers are inserted into the STXM prior to use with radioactive materials so that if a ceramic window breaks, the radioactive material will be captured. The STXM is simultaneously pump-purged with He to avoid pulling vacuum on the sample packages.

Results and discussion

Figure 1 shows the on-resonance absorption contrast images taken at the corresponding peak energies in Table 1 along with the $4d_{5/2}$ NEXAFS spectra recorded from particles with nominal compositions of UO_2, NpO_2, and PuO_2, respectively. The NEXAFS transition from the actinide $4d_{5/2}$ initial state is to the 5f states. Depending on Z, the corresponding transition energies are separated from their $4d_{3/2}$ spin-orbit partners by 40–50 eV (not shown). The Np and Pu dioxide spectra are the first NEXAFS obtained by spectromicroscopy from transuranic particulates in the soft X-ray energy region at these absorption edges. The NEXAFS spectra are the average absorption from a selected two-dimensional projection into the three-dimensional particle. A summary of the experimentally derived parameters for the actinide $4d_{5/2}$ edges obtained in these initial investigations and reference information are summarized in Table 1. The absorption features of the three actinide dioxides are of Lorentzian lineshape. The NEXAFS measurements have been successfully repeated for all of the actinide dioxide particles and are reproducible.

There are no experimental actinide dioxide NEXAFS results for these absorption thresholds in the literature, to the best of our knowledge. There have been studies of metallic uranium and several uranium compounds at the 4d edges (except for UO_2), as well as for metallic plutonium [19, 20]. A useful comparison is to the actinide metallic counterparts of the dioxides at the $4d_{5/2}$ edge from these studies. There is general agreement with the current results compared to α-U and α-Pu as summarized in Table 1. Note that in all cases, the NEXAFS features recorded with the STXM are about 0.6 eV narrower than the corresponding metallic features. This result may be related to actinide metal versus actinide dioxide considerations in which the differences in band structures lead to features with different widths. This has been observed in the NEXAFS of transition metals and

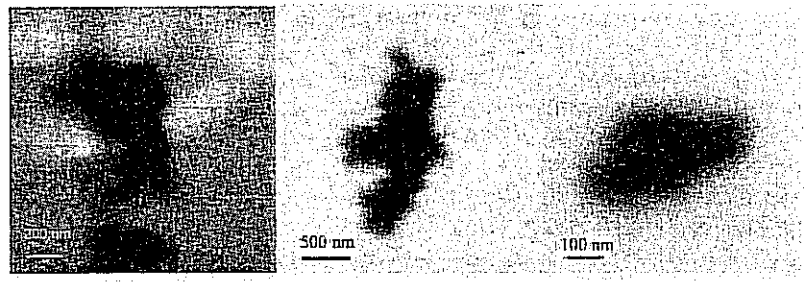

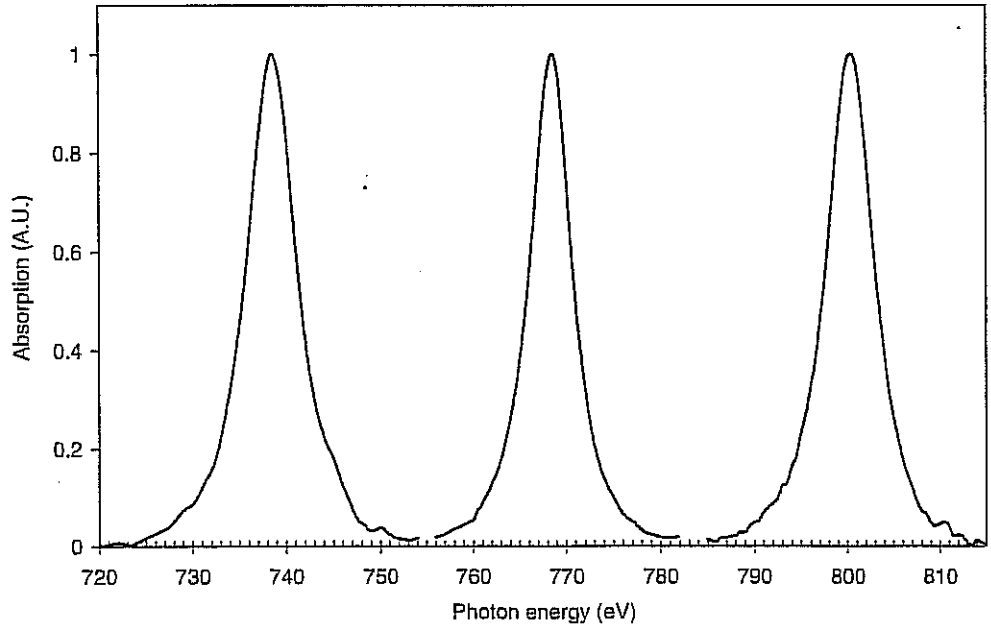

Fig. 1 Normal contrast images and NEXAFS spectra at the actinide $4d_{5/2}$ (N_5) edges of three actinide particles displayed omitting the $4d_{3/2}$ (N_4) edges. The compounds are, from *left* to *right*, uranium dioxide, neptunium dioxide, and plutonium dioxide, respectively

Table 1 Summary of parameters derived from the NEXAFS spectra of the actinide particles investigated in this study and the available reference information

Material	$4d_{5/2}$ reference energy (eV)[c]	$4d_{5/2}$ experimental energy (eV)	$4d_{5/2}$ experimental FWHM (eV)	$5d_{5/2}$, $5d_{3/2}$ reference energy (eV)[c]
U	737	736.4[d]	6.9 [d]	95, 104
UO_2[a]	–	738.5	6.3	–
Np	771	–	–	101, 109
NpO_2[a]	–	768.5	5.3	–
Np(V,VI) salt[b]	–	769.1	5.8	–
Pu	798	798.3[e]	5.9–6.5[e]	102, 113
PuO_2[a]	–	800.5	5.3	–

[a]Nominal actinide dioxide compositions
[b]Particle composition is 25% Np(V) and 75% Np(VI)
[c]See ref. [17]
[d]See ref. [19]
[e]See ref. [20]

transition metal oxides [21]. The results are generally consistent with the literature for the actinide metals and provide additional support for the reliability of the actinide dioxide STXM measurements. An interesting result is that the UO_2 edge is markedly wider (approximately 1 eV) than either of the transuranic dioxide features. A mixture of oxidation states (e.g., some U_3O_8 or UO_3 in the UO_2) could lead to a broadening of the absorption feature.

The Np $4d_{5/2}$ NEXAFS spectrum recorded from the mixed oxidation Np salt is compared to that obtained from NpO_2 in Fig. 2. The spectrum from the Np(V,VI) salt is shifted to higher energy by approximately 0.6 eV and is slightly broadened in comparison to the NpO_2(IV) spectrum. It should be noted that the Np(V,VI) spectrum shown in Fig. 2 was obtained minimizing exposure to the beam by using short dwell times at each pixel, but a certain amount of beam damage cannot be avoided. Together with the evidence mentioned in the Experimental section, the inspection of the NEXAFS spectra in Fig. 2 indicates that the Np salt is composed of higher oxidation state Np solids, primarily Np(VI). However, care must be taken when interpreting the relative energy positions of the Np(IV), Np(V), and Np(VI) features. The effective charge on the Np core may have subtle effects since the Np(V) and Np(VI) cores are neptunyl (O=Np=O) and this must be balanced against NpO_2 that has a significant number of electron-withdrawing oxygens. A similar charge state shift consideration has been observed and documented in the L_3 X-ray absorption near-edge spectroscopy of actinide materials. For example, the L_3 edge energy of *trans*-dioxo Pu(V) was found to be about 1 eV lower than that of PuO_2 [22]. The charge state shift of about 0.6 eV between Np(IV) and primarily Np(VI) is fairly consistent with the approximately 1.3 eV observed between the U(IV) and U(VI) oxidation states [6]. Beam damage effects may also contribute to the observation of the small charge state shifts between the Np oxidation states.

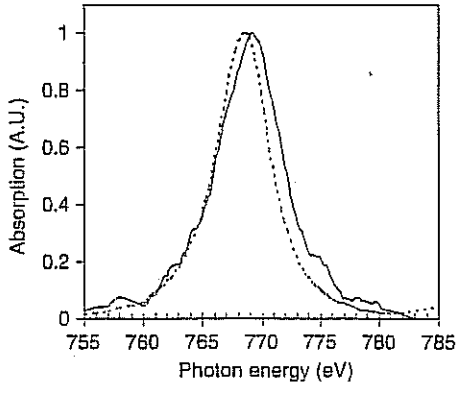

Fig. 2 Np $4d_{5/2}$ NEXAFS transmission spectra obtained from a mixed oxidation state Np(V,VI) salt (*dashed line*) compared to the NEXAFS spectrum from NpO_2 (*solid line*)

Figure 3 shows an image from the same Np(V,VI) salt particle where no countermeasures were taken to obviate radiation damage. It is clear, just from the image alone, that the particle is altered by exposure to the beam. The STXM NEXAFS linescan spectrum taken across the particle, resulting in the visible dark line, matches identically that obtained for NpO_2, verifying that reduction has occurred. For solid-state actinide materials, including the oxides, this is the first observation of routine beam damage that requires special data acquisition methods to preclude. This result also serves to further validate the relative energy positions of Np(IV) and Np(VI) features to one another, as well as the small charge state shift separating them.

Actinide elemental maps may be generated from two single-energy STXM images obtained at different energies, one at the actinide $4d_{5/2}$ edge maximum and one several eV below the edge. The images are first converted to optical density and then pixel-wise subtracted from each other yielding a map showing increased signal contrast where plutonium is present. A plutonium image on resonance and a plutonium elemental map obtained from a PuO_2 particle are shown in Fig. 4. The Pu $4d_{5/2}$ NEXAFS spectra were obtained from several different regions of the PuO_2 particle. Region-averaged NEXAFS spectra were constructed from the entire particle, the central region, and from the edge region alone (approximately 50 nm into the particle from the interface). All of the Pu $4d_{5/2}$ spectra appear the same. No beam-induced alteration was noted during the spec-

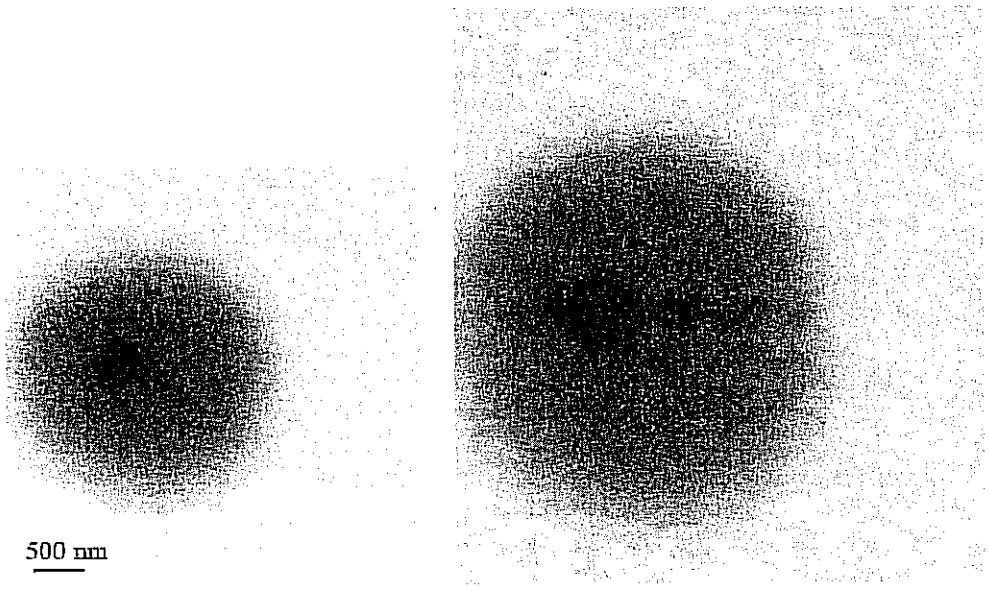

Fig. 3 Single-energy STXM images of a mixed oxidation Np(V,VI) salt particle. The *left image* shows the particle prior to a linescan across the center of the particle. There is clear evidence of radiation damage after the linescan in the image on the *right*. The *darker spot* near the *center* of the particle is due to earlier beam damage prior to collection of the unaltered spectrum. The size of the actual main particle is about 500 nm and the apparent size difference between the images is due to slightly different STXM focal settings

tromicroscopy of the PuO_2 particle. In a similar manner, chemical state or species-specific maps could also be obtained by contrasting specific NEXAFS spectral features, either actinide 4d or even oxygen K-edge, to one another.

The oxygen K-edge NEXAFS spectrum recorded from the UO_2 particle of Fig. 1 is shown in Fig. 5. There is a clear pre-edge feature located at about 532 eV, a shoulder on the main absorption threshold at 535 eV, and the main broad absorption manifold is centered around 540 eV. The oxygen K-edges have also been collected from several of the other common uranium oxide materials [23]. The spectromicroscopy NEXAFS spectrum agrees with those obtained by normal NEXAFS methods and theoretical calculations [24]. However, there are some slight differences in the pre-edge feature intensity and an oscillation at about 550 eV is not fully-resolved. It is possible that the slight loss of pre-edge feature intensity may be related to the transmission versus total electron yield detection modes.

Similar NEXAFS spectromicroscopy measurements have been recently made at the oxygen K-edges of the Np and Pu dioxides. For the case of NpO_2, initial oxygen K-edge extended X-ray absorption fine structure (EXAFS) has been obtained and the proper oscillations observed, although the signal-to-noise ratio needs improvement. The oxygen NEXAFS spectrum from NpO_2 is consistent with the electron energy loss spectroscopy (EELS) [25]. Oxygen K-edge NEXAFS spectra have also been collected from the PuO_2 particle of Fig. 4 at the same locations as the Pu $4d_{5/2}$ NEXAFS spectra. There is no spectral difference between the bulk-like regions. However, the edge region of the particle shows a marked difference in the pre-edge intensity relative to the main absorption feature.

One of the limitations of current actinide STXM investigations is the necessity to use the actinide 4d absorption edges for extracting chemical and electronic structure information. The absorption cross-section is small at these edges. The chemical shifts of the 4d edges, as mentioned in the Experimental section, are small and careful measurements are required. The electronic information obtainable from these 4d edges is valuable as this is not a commonly studied set of edges and can

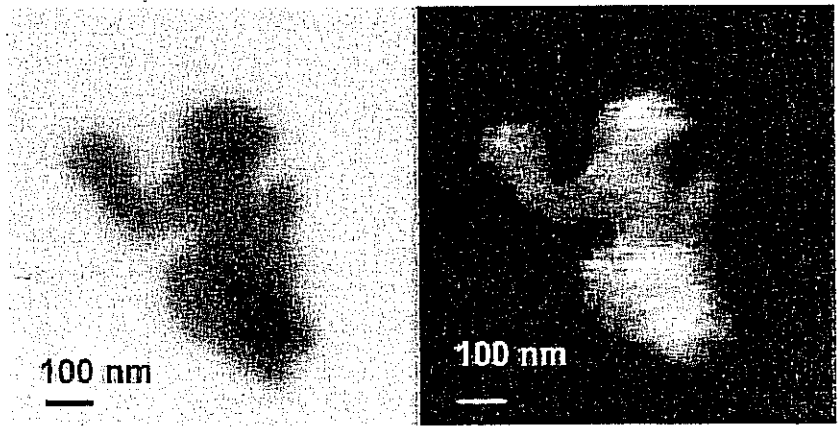

Fig. 4 Plutonium dioxide image (*left*) and the Pu elemental map (*right*) from a low-fired PuO_2 particle

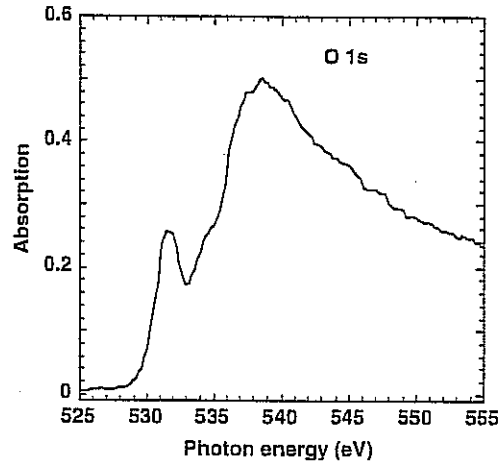

Fig. 5 Oxygen K-edge transmission NEXAFS spectrum collected from the UO_2 particle of Fig. 1

provide insight on 5f electron behavior [20]. There is no STXM, even the ALS-MES STXM, that can operate near or much below 120 eV to access the actinide 5d edges. With the actinide 5d as an objective, the capabilities to run the ALS-MES STXM at photon energies below the actinide 5d edges with a 40-nm zone plate are undergoing development. These most recent results are shown in Fig. 6, which depicts the monochromatized flux obtainable at the STXM end station without the Si_3N_4 sample windows required for actinide studies. This is the first operation of a STXM at such low energies. Use of the ceramic windows reduces the flux substantially (30% transmission each at about 100 eV) but leaves enough flux for effective measurements. Initial investigations at the 5d edge have shown some promise and primitive spectra have been recorded. Operation at the reduced flux level imposed by window operations poses complications since the amount of higher-order harmonics passed by the zone plate at these low energies,

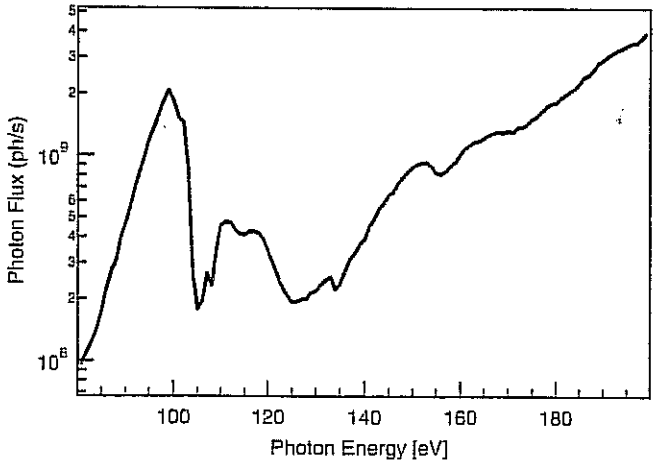

Fig. 6 Photon flux from the ALS-MES STXM documenting the first successful STXM at about 80 eV with a detector efficiency of about 10%

when operating the monochromator for maximum flux, is approaching the flux level of the selected primary X-ray beam energy.

Conclusions

Soft X-ray STXM spectromicroscopy at the ALS-MES beamline has been utilized for the first investigation of transuranic materials, and in particular, the actinide dioxides of uranium, neptunium, and plutonium. The capability to image and elementally map actinide elements enables the NEXAFS nanospectroscopy of the actinide particles. The capability to investigate different locations in particles will prove valuable in the future when inhomogeneous particles or systems are studied. The most useful actinide edge at this time for spectromicroscopy is the $4d_{5/2}$ edge, for both imaging and NEXAFS spectroscopy. The charge state shifts between oxidation states are small for the actinides at this edge but can be measured reproducibly at high resolution at the ALS-MES beamline, thus providing valuable information. The linewidths are narrower for the oxides and are consistent with what has been observed for metallic actinide systems. More thorough and complete investigations of fundamental, reference actinide materials that will follow in the future are necessary to fully establish the STXM spectromicroscopy of actinides. Although actinide dioxide particles are robust by STXM standards, the reduction of a mixed oxidation state Np(V,VI) particle was observed and special data acquisition precautions were implemented to avoid damage as much as possible. Oxygen K-edge NEXAFS spectra have been collected from the range of actinide dioxides and the UO_2 spectra are similar to those previously published for bulk materials. The use of the actinide 5d absorption edge requires more development, including the preparation of specially engineered thin samples, and may pose some complications when working with multi-component systems. However, it may effectively enable a most fundamental set of actinide experiments.

Soft X-ray STXM is a promising technique for the investigation of a range of actinide materials, particularly those with light element constituents, and is user-friendly in this energy region since it does not require a vacuum environment. Furthermore, the amount of actinide material required is small, which reduces safety concerns. Reaching its full potential depends on continued developments and the completion of fundamental actinide reference materials studies to fully define the complete capabilities of STXM actinide spectromicroscopy. For the investigation of actinide particulates, STXM is unique and will make contributions to science directly involved with small particles of actinides or in any system in which actinides are locally concentrated. Thus, STXM will be suitable for examining the distribution and speciation of actinides in several environmental and biosciences applications.

Acknowledgements This research, the ALS, and ALS-MES BL-11.0.2 are supported by the Director, Office of Science, Office of Basic Energy Sciences, Division of Chemical Sciences, Geosciences, and Biosciences and Materials Sciences Division of the US Department of Energy at the Lawrence Berkeley National Laboratory under Contract No. DE-AC03-76SF00098. The work was also partially supported by the Swedish Nuclear Fuel and Waste Management Company, SKB AB. REW was supported in part by the Office of Civilian Radioactive Waste Management Fellowship Program administered by Oak Ridge Institute for Science and Education under a contract with the US Department of Energy and the Oak Ridge Associated Universities. The authors are grateful to Brian S. Fairchild of LBNL EH&S for his assistance in the performance of the actinide STXM experiments.

References

1. Denlinger JD, Rotenberg E, Warwick T, Visser G, Nordgren J, Guo J-H, Skytt P, Kevan SD, McCutcheon KS, Tobin JG, Shuh DK, Bucher JJ, Edelstein NM, Tonner BP (1995) Rev Sci Instrum 66:1342–1345
2. Terry J, Schulze RK, Lashley J, Farr JD, Zocco T, Heinzelman K, Rotenberg E, Shuh DK, Van der Laan G, Tobin JG (2002) Surf Sci 499:L141–L147
3. Tobin JG, Chung BW, Wadddill GD, Schulze RK, Terry J, Farr JD, Zocco T, Shuh DK, Heinzelman K, Rotenberg E, Van der Laan G (2003) Phys Rev B 68:155109
4. Moore KT, Wall MA, Schwartz AJ, Chung BW, Shuh DK, Schulze RK, Tobin JG, (2003) Phys Rev Lett 90:196064
5. Shuh DK, Butorin SM, Guo J-H, Nordgren J (2004) Mater Res Soc Symp Proc 802:131–136
6. Bluhm H, Andersson K, Araki T, Benzerara K, Brown GE Jr, Dynes JJ, Ghosal S, Hansen H-Ch, Hemminger JC, Hitchcock AP, Ketteler G, Kneedler E, Lawrence JR, Leppard GG, Majzlam J, Mun BS, Myneni SCB, Nilsson A, Ogasawara H, Ogletree DF, Pecher K, Shuh DK, Salmeron M, Tonner B, Tyliszczak T, Yoon TH (2005) J Electron Spectr (in press)
7. Sharmasarkar S, Traina SJ, Tyliszczak T, Nilsson HJ, Shuh DK, in preparation (2005)
8. Stohr J (1992) NEXAFS spectroscopy. Springer series in surface science 25, Springer-Verlag, Berlin Heidelberg New York
9. Kilcoyne ALD, Tyliszczak T, Steele WF, Fakra S, Hitchcock P, Franck K, Anderson E, Harteneck B, Rightor EG, Mitchell GE, Hitchcock AP, Yang L, Warwick T, Ade H (2003) J Synch Rad 10:125
10. Coonley MS (2004) (ed) Actinide oxides I and II. Actinide research quarterly 2 and 3, Nucl Mat Tech Div, Los Alamos National Laboratory, Los Alamos, NM, USA
11. Wu ZY, Jollet F, Gota S, Thromat N, Gautier-Soyer M, Petit T (1999) J Phys Condens Matter 11:7185–7194
12. Tyliszczak T, Warwick T, Kilcoyne ALD, Fakra S, Shuh DK, Yoon TH, Brown GE Jr, Andrews S, Chembrolu V, Strachan J, Acremann Y (2004) Synch Rad Instrum 2003. AIP Conf Proc 705:1356–1359
13. Kilcoyne ALD, Tyliszczak T (2004) Synch Rad Instrum 2003. AIP Conf Proc 705:605–607
14. Harteneck BD, Olynick DL, Veklerov E, Tendulkar M, Liddle JA, Kilcoyne ALD, Tyliszczak T (2004) J Vac Sci Technol B 22:3186–3190
15. Advanced Light Source Molecular Science Beamline Webpages, LBN L, Berkeley, CA, (2005); http://beamline1102.als-lbl.gov/; http://www-als.lbl.gov/als/techspecs/bl11.0.2.html
16. Hitchcock AP (2004) Axis Version 21q (09-June-04). McMaster University, Hamilton ON Canada
17. Browne E, Firestone RB (1986) In: Shirley VS (ed) Table of radioactive isotopes. Wiley, New York, pp C14–C16
18. Center for X-ray optics, X-ray Interactions with Matter, LBNL, Berkeley, CA, USA; http://www-cxro.lbl.gov/optical_constants
19. Kalkowski G, Kaindl G, Brewer WD, Krone W (1987) Phys Rev B 35:2667–2677
20. Van der Laan G, Moore KT, Tobin JG, Chung BW, Wall MA, Schwartz AJ (2004) Phys Rev Lett 93:097401
21. de Groot FMF (1991) PhD Thesis, X-ray absorption of transition metal oxides. University of Nijmegen, Nijmegen, The Netherlands
22. Conradson SD, Abney KD, Begg BD, Brady ED, Clark DL, den Awer C, Ding M, Dorhout PK, Espinosa-Faller FJ, Gordon PJ, Haire RJ, Hess NJ, Hess RF, Keough DW, Lander GH, Lupinetti AJ, Morales LA, Neu MP, Palmer PD, Paviet-Hartmann P, Reilly SD, Runde WH, Tait CD, Veirs DK, Wastin F (2004) Inorg Chem 43:116–131
23. Tyliszczak T, Nilsson HJ, Nachimuthu P, Shuh DK (2005) unpublished experimental results
24. Jollet F, Petit T, Gota S, Thromat N, Gautier-Soyer M, Pasturel A (1997) J Phys Condens Matter 9:9393–9401
25. Buck EC, Colella M, Smith KL, Lumpkin GR (2002) Mat Res Soc Symp Proc 713:655–662